Author Manuscript

Author Manuscript

Author Manuscript

Author Manuscript

HHS Public Access

Author manuscript

Cancer J. Author manuscript; available in PMC 2016 March 01.

Published in final edited form as:

Cancer J. 2015 ; 21(2): 123–128. doi:10.1097/PPO.0000000000000097.

Imaging Tumor Metabolism using *in vivo* MR Spectroscopy

Yan Li, PhD[*], **Ilwoo Park, PhD**, and **Sarah J Nelson, PhD**

Department of Radiology and Biomedical Imaging, University of California, San Francisco, CA

Abstract

Magnetic resonance spectroscopy (MRS) is a powerful tool for noninvasively investigating normal and abnormal metabolism. When used in combination with imaging strategies, multi-nuclear MRS methods provide detailed biochemical information that can be directly correlated with anatomical features. Hyperpolarized ^{13}C MRS is a new technology that reflects real-time metabolic conversion and is likely to be extremely valuable in managing patients with cancer. This article reviews the use of *in vivo* ^{31}P, ^{1}H, and ^{13}C MRS for assessing cancer metabolism in order to provide information for diagnosis, planning treatment, assessing response to therapy, and predicting survival for patients with cancer.

Keywords

magnetic resonance spectroscopy; hyperpolarization; tumor; cancer metabolism

It is almost a century ago since Warburg pointed out that cancer cells have different metabolism from normal cells. Decades of studies that have focused on oncogenic pathways for tumorgenesis have established a clear relationship between malignant transformation, response to treatment and changes in metabolism. Although the interactions between these processes are complex, the ability to serially monitor such biochemical processes within morphologically heterogeneous tumors is of great significance for managing patients with cancer. Locating regions that are either metabolic active, show hypoxia or correspond to treatment-related effects is critical for determining at an early stage whether patients are responding to therapy or whether a new treatment strategy should be considered. *In vivo* magnetic resonance spectroscopy (MRS) is a powerful tool for non-invasively investigating normal and abnormal metabolism. Although many of the initial studies in oncology focused on using MRS for pre-clinical investigations, there is a substantial literature in applying this technology to patients with cancer.

Important applications of MRS are in providing information for diagnosis, directing image-guided surgery and radiation planning, and predicting survival in single-voxel and multi-voxel (also called magnetic resonance spectroscopic imaging, MRSI) acquisition modes. With proper strategies of implementing fast spectroscopic imaging techniques, the latter allows the spatial extent of abnormal metabolic properties to be characterized within a clinically reasonable total acquisition time of 5-10 minutes [1]. The recent availability of 7T

[*] Corresponding Author: Yan Li, PhD UCSF Radiology Box 2532 1700 4th Street, Byers Hall 301 San Francisco, CA 94158-2532 Tel: (415) 514-4419 Fax: (415) 514-1028 yan.li@ucsf.edu.

Author Manuscript Author Manuscript Author Manuscript Author Manuscript

whole body MR scanners offers advantages in higher signal-to-noise ratio and enhanced spectra quantification [2], can be used to improve the spatial resolution and detection of a wider range of metabolites. The MRS signal is based on the interaction between atom nuclei and an external magnetic field. The most common nuclei that have been applied are phosphorus (^{31}P), proton (^{1}H), and carbon (^{13}C). Differences on chemical shift and J-coupling in molecules allow for the identification of different chemical compounds. In this review, we discuss the application of MRS in the terms of the commonly used nuclei. While our main focus is on patients with brain tumors, it should be noted that similar studies have been applied to cancers in the prostate, breast and musculoskeletal system.

Phosphorus-31 (^{31}P) Magnetic Resonance Spectroscopy

^{31}P MRS has been used to assess phosphorus metabolism. The main metabolite markers are phosphomonoesters (phosphocholine (PC) and phosphoethanolamine (PE)), phosphodiesters (glycerophosphocholine (GPC) and glycerophosphoethanolamine (GPE)), phosphocreatine (PCr), alpha adenosine triphosphate (α-ATP), β-ATP, γ-ATP and inorganic phosphate (Pi). The intracellular pH can also be determined by the chemical shift between Pi and PCr. The main findings in early studies that used ^{31}P MRS were that PC is elevated in most aggressive tumors and that changes in the levels of PC, PE, GPC and GPE are associated with response to therapy [3, 4]. Changes in levels of PCr and elevation of pH have been found in patients with brain and other tumors [5], but, overall, the results have been limited by a relatively low spatial resolution and tumor heterogeneity. This makes it difficult for interpretation of the data and has limited the number of applications in the clinic to a small number of research groups who are using high field scanners. On the other hand, its central role in monitoring energy metabolism means that ^{31}P MRS remains a critical tool for investigating tumor metabolism in both cell and pre-clinical model systems [6, 7].

Proton (^{1}H) Magnetic Resonance Spectroscopy

^{1}H MRS is more widely used for the studying patients with cancer because of the development of improved acquisition techniques and its natural and biological abundance. In this case the predominant water and the lipid outside the volume of interested need to be suppressed for the detection of the weaker signals from metabolites. Choline containing compounds (Cho), creatine (Cr), N-acetyl aspartate (NAA), lactate (Lac) and Lipid (Lip) (Figure 1) are the major metabolites in brain spectra that are acquired with long echo time (>130ms), which is the most commonly used acquisition method in neuro-oncology. The elevation of Cho, due to increased membrane synthesis in neoplasms, and the reduction of the neuronal marker NAA have been used for distinguishing regions of tumor from normal brain tissue [8]. The Cho peak from *in vivo* spectra at 1.5T and 3T represents Cho, PC and GPC. A switch from GPC to PC was found to associate with glioma malignancy [9]. Cr and PCr are involved in ATP metabolism, and altered levels of total Cr have been reported in glioma [10]. Lac, which is a marker of anaerobic metabolism, overlaps with Lip signals that arise from necrosis or from contamination due to subcutaneous Lip. Spectral editing using J-difference methods have been applied to separate Lac from Lip for assessing the malignancy of tumors [11] (Figure 1). High levels of Lac and Lip have been reported as a robust predictor of poor overall survival in patients with glioblastoma [12].

Author Manuscript Author Manuscript Author Manuscript Author Manuscript

Results from the analysis of image-guided tissue samples using *ex vivo* ^{1}H high-resolution magic-angle-spinning nuclear magnetic resonance (HRMAS-NMR) spectroscopy have shown the potential roles of other metabolites, such as myo-inositol (mI), glutamate (Glu), glutamine (Gln) and glutathione (GSH), in differentiating between tumor and gliosis, and/or associating with malignant transformation [13, 14], which provides strong motivation for performing *in vivo* short echo (<40ms) MRS studies in patients with glioma. At short echo time, the contrast between tumor and normal tissues in MRS data are different from the long echo time spectra because of differential increase in T2 relaxation time for Cho and Cr relative to NAA [10]. Not only do the metabolites with low concentration and/or complex coupling patterns appear in short echo time MRS, but the magnitudes of water and lipid are also increased. Improved water and lipid suppression are therefore required for obtaining reliable short echo MRS data.

An example of spectra acquired using short echo MRSI at 3T is illustrated in Figure 2A. The mI is predominantly located within astrocytes, and often overlaps with the peak of glycine in spectrum. Elevations in mI and glycine were observed in low-grade but shown to decrease in high-grade brain tumor lesions [15]. From *ex vivo* tissue samples, it has been proposed that mI/Cho is of interest for differentiating between tumor and gliosis [14]. Glu and Gln also appear in the spectrum but the peak overlapping makes it difficult to isolate individual components at 1.5T or 3T, thus a combined index known as Glx that represents a combination of Glu and Gln is often used for comparative purpose. Gln, a precursor for Glu and GSH, participates in energy metabolism, macromolecular synthesis and signaling pathways [16], suggesting that it is a good target to treat or monitor patients [17]. Glu is the main excitatory neuro-transmitter in the brain, and glioma cells have been found to secret Glu resulting in an increase in extra-cellular Glu [18]. GSH is an antitoxidant that prevents damage from reactive oxygen species and it can be detected using spectral editing MRS sequences or at higher field strength. The complex roles of Glu, Gln, and GSH in tumors make it valuable for evaluation of patients with glioma.

Mutations in isocitrate dehydrogenase (IDH) enzymes were recently found in more than 70% of patients with low-grade glioma and secondary glioblastoma [19], and the presence of mutations is associated with longer overall survival [20, 21]. The onco-metabolite, 2-hydroxygluatarate (2-HG), is associated with presence of IDH1 mutations [22]. 2-HG can be detected using *in vivo* MRS acquisitions at 3T [23]. Figure 3 shows an example of spectra acquired from a patient with grade 2 glioma and IDH1 mutations. Based on the significant role on predicting overall survival and the spectral results from *ex vivo* tissue samples on malignant transformation [13], it is anticipated that evaluating 2-HG in patients with glioma will be of great significance in the patient management.

Although there are some engineering issues that make the implementation of MRS at high field scanners more challenging for patient studies, improving the sensitivity of MRS and increasing the number of metabolites that can be assessed is an important advance for evaluating patients with cancer. Figure 2B shows an example of *in vivo* 3D MRSI data at 7T from a patient with glioblastoma. The previous application of short echo time 3D MRSI in patients with glioma at 7T showed significantly increased levels of Cho, Gln, mI, Gly and GSH relatively to Cr and decreased NAA for regions of tumor versus normal brain [24]. The

Author Manuscript Author Manuscript Author Manuscript Author Manuscript

comparisons on reliability and practicality of using 7T relative to the more standard 3T scanner for assessing tumor would be important in planning the data acquisition for the cancer studies.

The acquisition methods and clinical applications of MRS to patients with prostate cancer are similar in nature to those in patients with brain tumors. In that case Cho, Cr, polyamine and citrate are the relevant metabolic markers. In a healthy prostate, epithelial cells have high levels of polyamine, and relatively high concentration of citrate can be found in the glandular tissue. As was the case with brain tumors, the level of Cho is elevated in prostate cancer, while citrate and polyamine peaks are decreased. The variations in concentrations of these metabolites have been used for localizing the tumor, determining tumor grades, planning treatment, and evaluating response to therapy [25].

Carbon-13 (^{13}C) Magnetic Resonance Spectroscopy

Cancers preferentially reply on non-oxidative glycolysis for energy production, and excess lactate is produced as a result [26]. Although ^{1}H MRS has been one of the major tools used to non-invasively detect lactate in tumor, it can be technically challenging due to overlapping lipid resonances. Positron emission tomography (PET) imaging with 2-[^{18}F]fluoro-2-deoxy-D-glucose (FDG) is used to monitor uptake of FDG in tumors, with a particular emphasis on detecting metastases using whole body screens. Despite its high sensitivity and appealing potential for assisting in diagnosis and management of other cancers, the high levels of FDG uptake in normal grey matter have similarly limited its application in clinical neuro-oncology. Although ^{13}C MRS has previously been used to study *in vivo* tumor metabolism, the intrinsically low concentration of cellular metabolites in the body that are labeled with ^{13}C nuclei and the consequently low sensitivity compared to ^{1}H MRS have, until recently, limited the applications of this technique in the clinic.

Dynamic Nuclear Polarization (DNP) and the development of a dissolution process which retains polarization into the liquid state for long enough to enable the real time investigation of *in vivo* metabolism can provide more than 10,000-fold signal increase over conventional ^{13}C methods [27]. Tumors frequently have high levels of lactate dehydrogenase A (LDH-A), (which preferentially converts pyruvate to lactate) and NADH, the co-factor required for LDH-A activity, both of which play a role in the high levels of lactate observed in many tumors [28]. Based on these observations, the administration of hyperpolarized compounds such as ^{13}C-labeled pyruvate to tumor-bearing subjects, followed by the real-time monitoring of conversion of the substrate to various labeled metabolites using ^{13}C MRSI have shown the potential of this technique as a unique non-invasive tool for imaging tumor metabolism. Initial studies have shown that with an injection of hyperpolarized [1-^{13}C]-pyruvate into rats and pigs, both the substrate and its metabolic products [1-^{13}C]-alanine [1-^{13}C]-lactate can be observed in tissues of interest [29]. Further work has suggested that the approach could also be used to study drug response because cells undergoing growth arrest or apoptosis convert less hyperpolarized pyruvate to lactate [30]. More recently, the increased conversion of hyperpolarized pyruvate to lactate was shown to precede the onset of tumor growth, and also was reversed prior to tumor regression, at least in a myc-driven murine model of liver cancer [31].

Author Manuscript Author Manuscript Author Manuscript Author Manuscript

A number of studies in brain tumor models have used hyperpolarized [1-^{13}C]-pyruvate as a substrate to demonstrated its utility as a tool for examining *in vivo* tumor metabolism [32, 33]. These pre-clinical studies have shown that it is able to differentiate tumor from normal brain tissue, characterize ^{13}C metabolite patterns between pathologically heterogeneous abnormal and normal brain tissue, as well as detect early response to treatment in animal models of high-grade gliomas. In a recent study, changes in pyruvate metabolism following injection of hyperpolarized [1-^{13}C]-pyruvate was shown to be linked to Temozolomide (TMZ)-induced DNA damage, and therefore, to be exploited by ^{13}C MRSI as an early sensor of TMZ therapeutic response [34]. This is likely to be extremely important as TMZ is a key component of the standard of care treatment for patients with high grade glioma.

The first clinical trial that used hyperpolarized ^{13}C MR metabolic imaging was performed in patients with prostate cancer [35] (Figure 4). This study showed that there were no dose limiting toxicities following an injection of hyperpolarized [1-^{13}C]-pyruvate and demonstrated elevated [1-^{13}C]-lactate/[1-^{13}C]-pyruvate in regions of biopsy-proven cancer. These findings will be valuable for noninvasive cancer diagnosis and treatment monitoring in future clinical trials and suggests that hyperpolarized ^{13}C MRSI is likely to be a promising tool for monitoring tumor growth and tumor drug response.

Conclusion

In summary, we have described the use of *in vivo* ^{31}P, ^{1}H, and ^{13}C MRS as non-invasive methods for assessing cancer metabolism. When combined with standard MR imaging techniques that visualize changes in morphological abnormalities, MRS provides biochemical information that can be directly correlated with regions of the anatomy. The hyperpolarized ^{13}C MRS is even more promising for obtaining real-time metabolic conversion in the tumor lesion. These are of great significance in monitoring response to therapy, evaluating tumor progression and possibly tailoring treatment to the characteristics of each individual tumor. Although applications in brain and prostate were mainly discussed here, this method is applicable and has been used in many other cancer studies (eg. [36]). Despite increasing interest in the use of MRS, this technology is still limited in terms of the acquisition and analysis tools available on commercial MR scanners. Achieving higher SNR, better spatial resolution and improved metabolite quantification will be the focus for future patient studies in order to make a compelling case for further development.

Glossary

^{1}H	proton
^{13}C	carbon-13
^{31}P	phosphorus-31
2-HG	2-hydroxygluatarte
ATP	adenosine triphosphate
Cho	choline containing compounds

Author Manuscript Author Manuscript Author Manuscript Author Manuscript

Cr	creatine
DNP	dynamic nuclear polarization
FDG	2-[^{18}F]fluoro-2-deoxy-D-glucose
GPC	glycerophosphocholine
GPE	glycerophosphoethanolamine
HRMAS	high-resolution magic-angle-spinning
IDH	isocitrate dehydrogenase
Lac	lactate
LDH	lactate dehydrogenase
Lip	lipid
Glu	glutamate
Gln	glutamine
GSH	glutathione
mI	myo-inositol
MRS	magnetic resonance spectroscopy
MRSI	magnetic resonance spectroscopic imaging
NAA	N-acetyl aspartate
NMR	nuclear magnetic resonance
PC	phosphocholine
PCr	phosphocreatine
PE	phosphoethanolamine
PET	positron emission tomography
Pi	inorganic phosphate
TMZ	temozolomide

References

1. Nelson SJ, Ozhinsky E, Li Y, et al. Strategies for rapid in vivo 1H and hyperpolarized 13C MR spectroscopic imaging. J Magn Reson. 2013; 229:187–197. [PubMed: 23453759]
2. Mekle R, Mlynarik V, Gambarota G, et al. MR spectroscopy of the human brain with enhanced signal intensity at ultrashort echo times on a clinical platform at 3T and 7T. Magn Reson Med. 2009; 61:1279–1285. [PubMed: 19319893]
3. Dewhirst MW, Sostman HD, Leopold KA, et al. Soft-tissue sarcomas: MR imaging and MR spectroscopy for prognosis and therapy monitoring. Work in progress. Radiology. 1990; 174:847–853. [PubMed: 2154837]
4. Griffiths JR, Cady E, Edwards RH, et al. 31P-NMR studies of a human tumour in situ. Lancet. 1983; 1:1435–1436. [PubMed: 6134191]

Author Manuscript Author Manuscript Author Manuscript Author Manuscript

5. Miyamachi K, Abe H, Miyasaka K. [Phosphorus-31 MR spectroscopy of brain tumors]. No Shinkei Geka. 1990; 18:533–537. [PubMed: 2395512]
6. Dewhirst MW, Poulson JM, Yu D, et al. Relation between pO2, 31P magnetic resonance spectroscopy parameters and treatment outcome in patients with high-grade soft tissue sarcomas treated with thermoradiotherapy. Int J Radiat Oncol Biol Phys. 2005; 61:480–491. [PubMed: 15667971]
7. Lora-Michiels M, Yu D, Sanders L, et al. Extracellular pH and P-31 magnetic resonance spectroscopic variables are related to outcome in canine soft tissue sarcomas treated with thermoradiotherapy. Clin Cancer Res. 2006; 12:5733–5740. [PubMed: 17020978]
8. McKnight TR, Noworolski SM, Vigneron DB, et al. An automated technique for the quantitative assessment of 3D-MRSI data from patients with glioma. J Magn Reson Imaging. 2001; 13:167–177. [PubMed: 11169821]
9. Aboagye EO, Bhujwalla ZM. Malignant transformation alters membrane choline phospholipid metabolism of human mammary epithelial cells. Cancer Res. 1999; 59:80–84. [PubMed: 9892190]
10. Li Y, Srinivasan R, Ratiney H, et al. Comparison of T(1) and T(2) metabolite relaxation times in glioma and normal brain at 3T. J Magn Reson Imaging. 2008; 28:342–350. [PubMed: 18666155]
11. Park I, Chen AP, Zierhut ML, et al. Implementation of 3 T lactate-edited 3D 1H MR spectroscopic imaging with flyback echo-planar readout for gliomas patients. Ann Biomed Eng. 2011; 39:193–204. [PubMed: 20652745]
12. Li Y, Lupo JM, Parvataneni R, et al. Survival analysis in patients with newly diagnosed glioblastoma using pre- and postradiotherapy MR spectroscopic imaging. Neuro Oncol. 2013; 15:607–617. [PubMed: 23393206]
13. Elkhaled A, Jalbert L, Constantin A, et al. Characterization of metabolites in infiltrating gliomas using ex vivo (1)H high-resolution magic angle spinning spectroscopy. NMR Biomed. 2014; 27:578–593. [PubMed: 24596146]
14. Srinivasan R, Phillips JJ, Vandenberg SR, et al. Ex vivo MR spectroscopic measure differentiates tumor from treatment effects in GBM. Neuro Oncol. 2010; 12:1152–1161. [PubMed: 20647244]
15. Castillo M, Smith JK, Kwock L. Correlation of myo-inositol levels and grading of cerebral astrocytomas. AJNR Am J Neuroradiol. 2000; 21:1645–1649. [PubMed: 11039343]
16. Hensley CT, Wasti AT, DeBerardinis RJ. Glutamine and cancer: cell biology, physiology, and clinical opportunities. J Clin Invest. 2013; 123:3678–3684. [PubMed: 23999442]
17. Wise DR, Thompson CB. Glutamine addiction: a new therapeutic target in cancer. Trends Biochem Sci. 2010; 35:427–433. [PubMed: 20570523]
18. Takano T, Lin JH, Arcuino G, et al. Glutamate release promotes growth of malignant gliomas. Nat Med. 2001; 7:1010–1015. [PubMed: 11533703]
19. Yan H, Parsons DW, Jin G, et al. IDH1 and IDH2 mutations in gliomas. N Engl J Med. 2009; 360:765–773. [PubMed: 19228619]
20. Sanson M, Marie Y, Paris S, et al. Isocitrate dehydrogenase 1 codon 132 mutation is an important prognostic biomarker in gliomas. J Clin Oncol. 2009; 27:4150–4154. [PubMed: 19636000]
21. Ohno M, Narita Y, Miyakita Y, et al. Secondary glioblastomas with IDH1/2 mutations have longer glioma history from preceding lower-grade gliomas. Brain Tumor Pathol. 2013; 30:224–232. [PubMed: 23494632]
22. Dang L, White DW, Gross S, et al. Cancer-associated IDH1 mutations produce 2-hydroxyglutarate. Nature. 2009; 462:739–744. [PubMed: 19935646]
23. Choi C, Ganji SK, DeBerardinis RJ, et al. 2-hydroxyglutarate detection by magnetic resonance spectroscopy in IDH-mutated patients with gliomas. Nat Med. 2012; 18:624–629. [PubMed: 22281806]
24. Li Y, Larson P, Chen AP, et al. Short-echo three-dimensional H-1 MR spectroscopic imaging of patients with glioma at 7 tesla for characterization of differences in metabolite levels. J Magn Reson Imaging. 2014
25. Kurhanewicz J, Vigneron DB. Advances in MR spectroscopy of the prostate. Magn Reson Imaging Clin N Am. 2008; 16:697–710, ix-x. [PubMed: 18926432]
26. Warburg O. On the origin of cancer cells. Science. 1956; 123:309–314. [PubMed: 13298683]

Author Manuscript Author Manuscript Author Manuscript Author Manuscript

27. Ardenkjaer-Larsen JH, Leach AM, Clarke N, et al. Dynamic nuclear polarization polarizer for sterile use intent. NMR Biomed. 2011; 24:927–932. [PubMed: 21416540]

28. Hirschhaeuser F, Sattler UG, Mueller-Klieser W. Lactate: a metabolic key player in cancer. Cancer Res. 2011; 71:6921–6925. [PubMed: 22084445]

29. Golman K, in 't Zandt R, Thaning M. Real-time metabolic imaging. Proc Natl Acad Sci U S A. 2006; 103:11270–11275. [PubMed: 16837573]

30. Day SE, Kettunen MI, Gallagher FA, et al. Detecting tumor response to treatment using hyperpolarized 13C magnetic resonance imaging and spectroscopy. Nat Med. 2007; 13:1382–1387. [PubMed: 17965722]

31. Hu S, Balakrishnan A, Bok RA, et al. 13C-pyruvate imaging reveals alterations in glycolysis that precede c-Myc-induced tumor formation and regression. Cell Metab. 2011; 14:131–142. [PubMed: 21723511]

32. Park I, Hu S, Bok R, et al. Evaluation of heterogeneous metabolic profile in an orthotopic human glioblastoma xenograft model using compressed sensing hyperpolarized 3D 13C magnetic resonance spectroscopic imaging. Magn Reson Med. 2013; 70:33–39. [PubMed: 22851374]

33. Park I, Bok R, Ozawa T, et al. Detection of early response to temozolomide treatment in brain tumors using hyperpolarized 13C MR metabolic imaging. J Magn Reson Imaging. 2011; 33:1284–1290. [PubMed: 21590996]

34. Park I, Mukherjee J, Ito M, et al. Changes in Pyruvate Metabolism Detected by Magnetic Resonance Imaging Are Linked to DNA Damage and Serve as a Sensor of Temozolomide Response in Glioblastoma Cells. Cancer Res. 2014

35. Nelson SJ, Kurhanewicz J, Vigneron DB, et al. Metabolic imaging of patients with prostate cancer using hyperpolarized [1-(1)(3)C]pyruvate. Sci Transl Med. 2013; 5:198ra108.

36. Shin HJ, Baek HM, Cha JH, et al. Evaluation of breast cancer using proton MR spectroscopy: total choline peak integral and signal-to-noise ratio as prognostic indicators. AJR Am J Roentgenol. 2012; 198:W488–497. [PubMed: 22528931]

Author Manuscript Author Manuscript Author Manuscript Author Manuscript

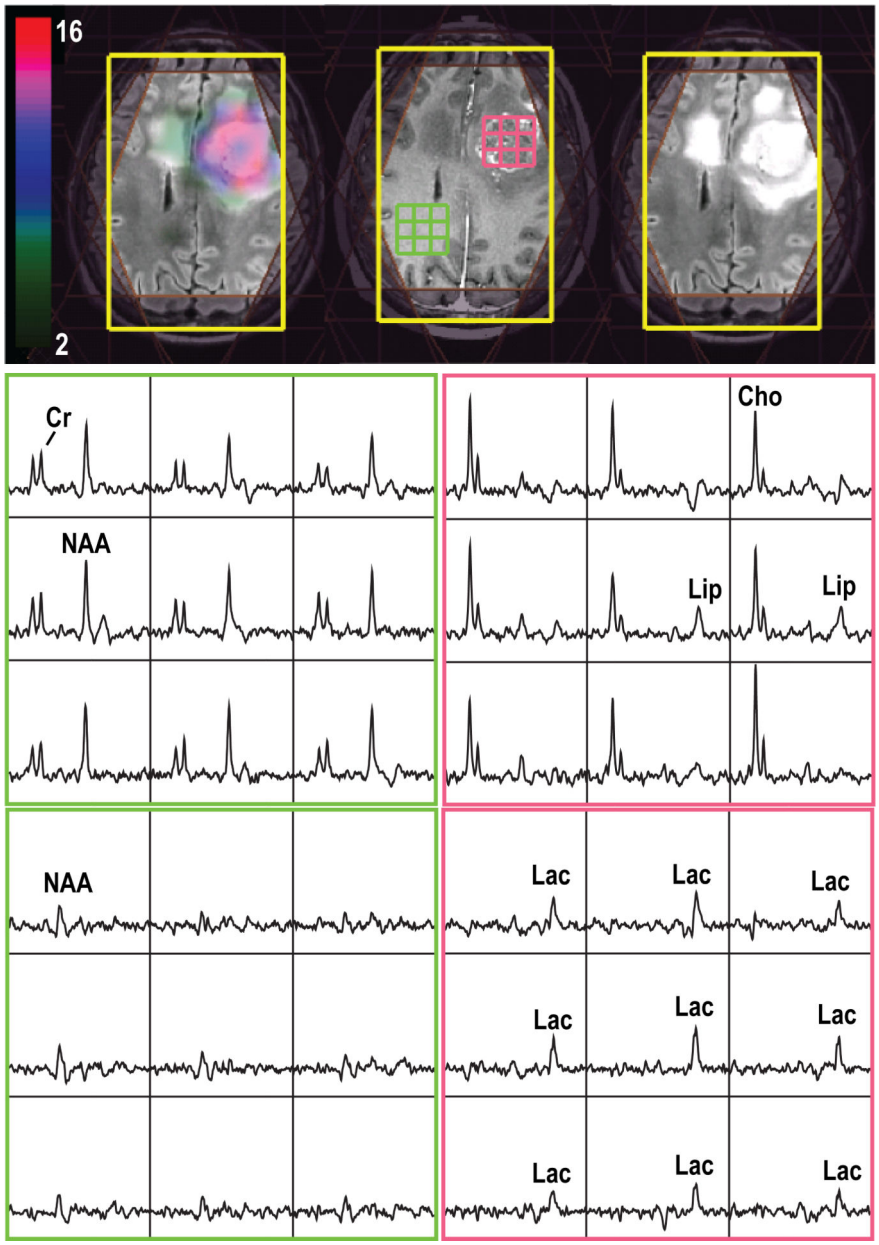

Figure 1.

3D Lac-edited ^{1}H MRSI acquired from a patient with a newly-diagnosed glioblastoma at the time of pre-treatment (TE/TR=144/1500ms, matrix size=18×18×16, elliptical sampling and flyback in S/I, nominal spatial resolution=1cm^{3}, 1 cycle edited on, 1 cycle edited off, total acquisition time=12.96min). Spectral array corresponded to summed (middle row) and difference (last row) of the Lac-edited spectra. The Cho-to-NAA index overlaid on T2-weighted images shows abnormal metabolic lesions.

Author Manuscript Author Manuscript Author Manuscript Author Manuscript

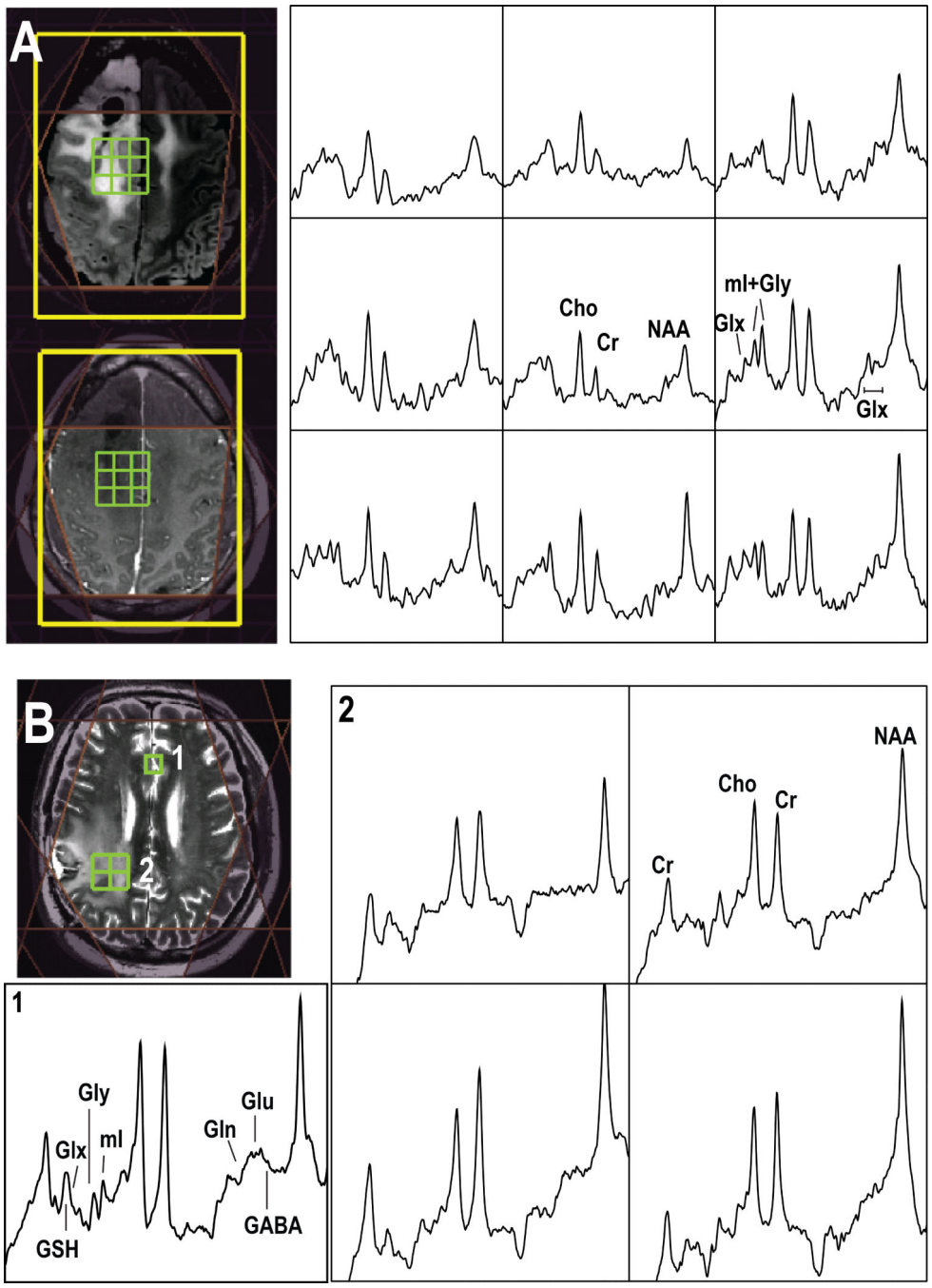

Figure 2.

Examples of short echo ^{1}H MRSI acquired from (A) a patient with grade 2 glioma at 3T (TE/TR=35/1500ms, matrix size=18×18×16, flyback in S/I, nominal spatial resolution=1cm^{3}, total acquisition time=8.1min) and (B) a patient with glioblastoma at 7T (TE/TR=30/2000ms, matrix size=18×22×8, flyback in A/P, nominal spatial resolution=1cm^{3}, total acquisition time=9.6min). Note the baseline has not been removed from the spectra that are shown.

Author Manuscript Author Manuscript Author Manuscript Author Manuscript

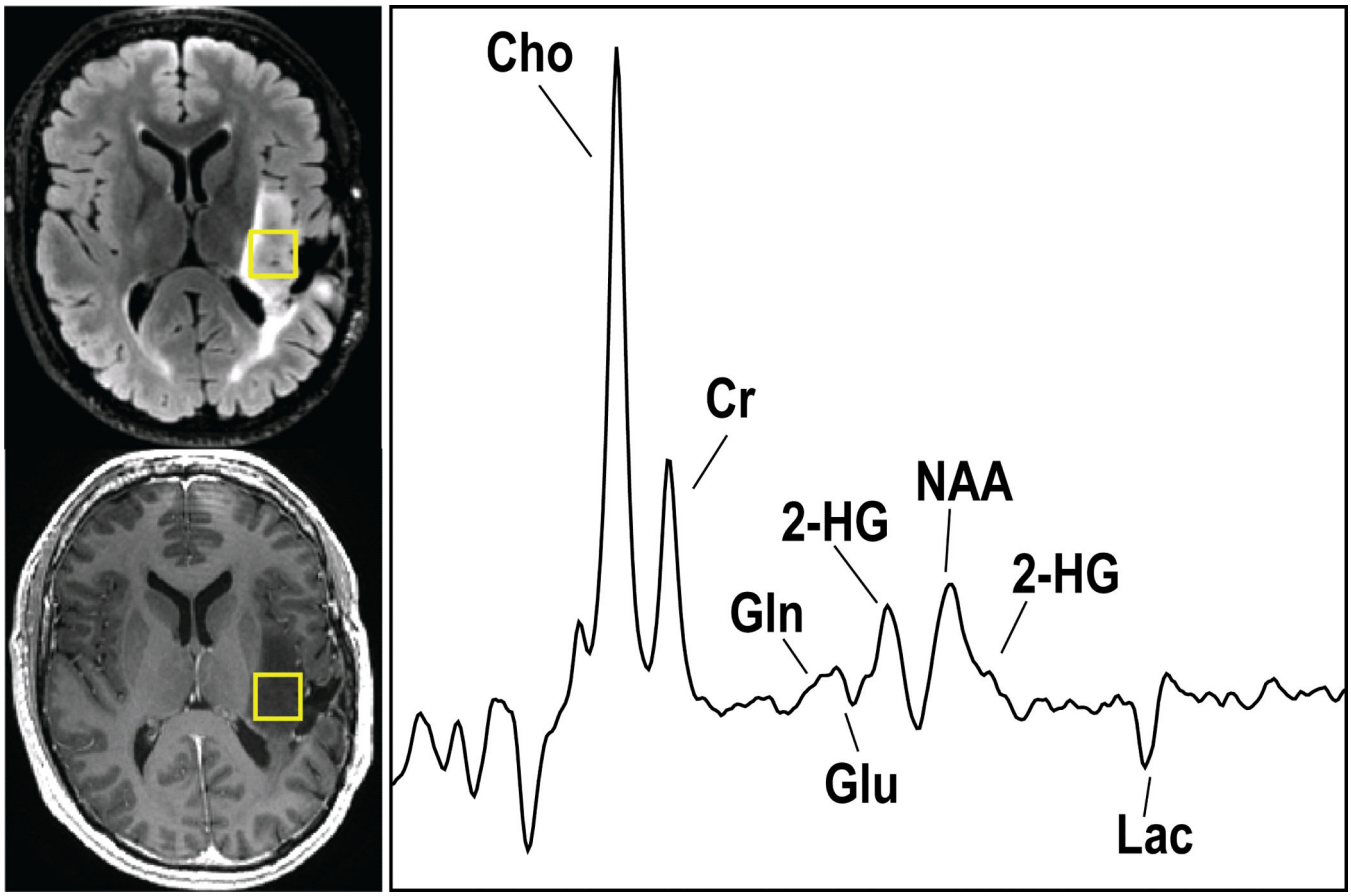

Figure 3.

Single-voxel ^{1}H spectra acquired from a patient with a grade 2 glioma and IDH1 mutations is able to detect *in vivo* 2-HG (TE1/TE2/TR=32/65/2000ms, voxel size=2×2×2 cm^3, 64 averaging, total acquisition time=2.80 min).

Author Manuscript Author Manuscript Author Manuscript Author Manuscript

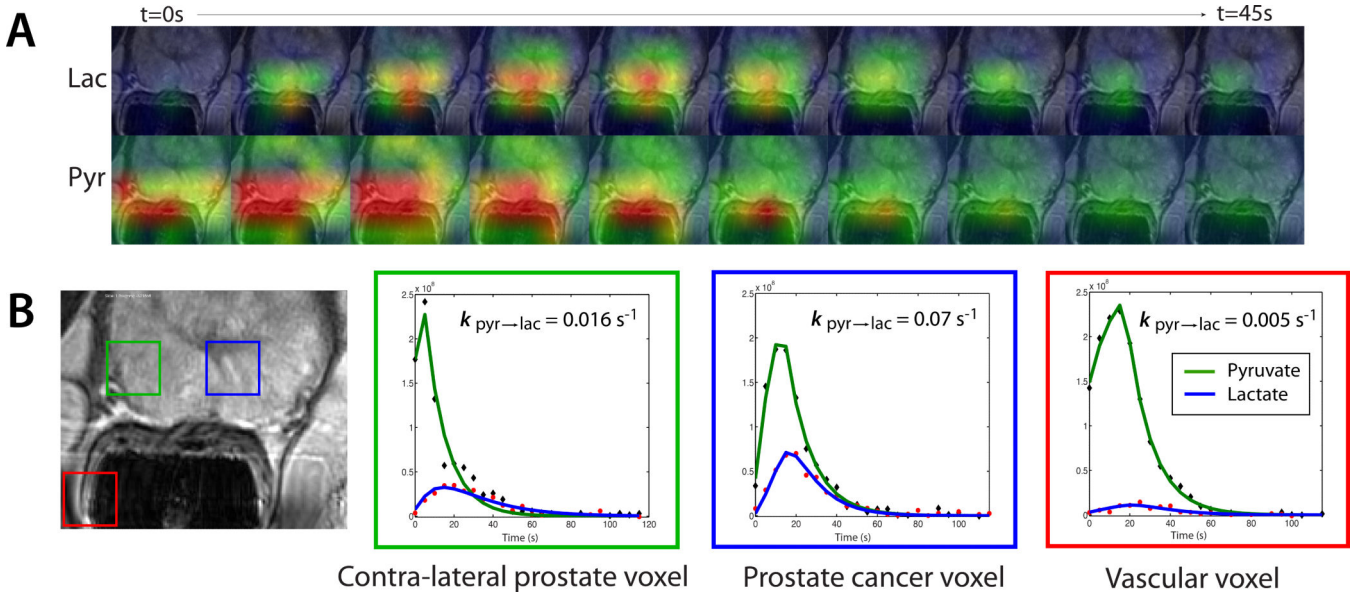

Figure 4.

2D ^{13}C dynamic MRSI data from a patient with biopsy-proven prostate cancer who received an injection of hyperpolarized [1-^{13}C]-pyruvate. (A) Lactate and pyruvate signal were acquired every 5 s. (B) A focus of mild hypointensity can be seen on the T2-weighted image (blue voxel). Dynamic pyruvate and lactate data from voxels overlapping the contralateral region of prostate (green), a region of prostate cancer (blue), and a vessel outside the prostate (red) were fit using a two-site exchange model [35].